ELSEVIER

Biochemical Pharmacology 61 (2001) 1463–1470

Biochemical Pharmacology

Azole-antifungal binding to a novel cytochrome P450 from *Mycobacterium tuberculosis*: implications for treatment of tuberculosis

Hebe M. Guardiola-Diaz[a,b,*], Lisa-Anne Foster[a], Darren Mushrush[a], Alfin D.N. Vaz[c,1]

[a]*Department of Biology, Trinity College, 300 Summit St., Hartford, CT 06106, USA*
[b]*Neuroscience Program, Trinity College, 300 Summit St., Hartford, CT 06106, USA*
[c]*Department of Biological Chemistry, University of Michigan Medical School, 1301 E. Catherine, Ann Arbor, MI 48109-0606, USA*

Received 24 April 2000; accepted 8 September 2000

Abstract

Although antibiotics against *Mycobacterium tuberculosis* have decreased the incidence of tuberculosis infections significantly, the emergence of drug-resistant strains of this deadly pathogen renders current treatments ineffective. Therefore, it is imperative to identify biochemical pathways in *M. tuberculosis* that can serve as targets for new anti-mycobacterial drugs. We recently cloned, expressed, and purified MT CYP51, a soluble protein from *M. tuberculosis* that is similar in sequence to CYP51 (lanosterol-14α-demethylase) isozymes, pharmacological targets for several anti-mycotic compounds. Its striking amino acid sequence similarity to that of mammalian and fungal CYP51s led to the hypothesis that MT CYP51 plays an important role in mycobacterial biology that can be targeted for drug action. In this manuscript, we established through spectral analysis that several azole antifungals bind MT CYP51 with high affinity. The effects of several azole compounds on the growth of *M. bovis* and *M. smegmatis*, two mycobacterial species that closely resemble *M. tuberculosis* were examined. We established a correlation between the affinity of azole compounds to MT CYP51 and their ability to impair the growth of *M. bovis* and *M. smegmatis*. These results suggest that the metabolic functions of MT CYP51 may be comparable to those of CYP51 in yeast and fungi and may lead to the development of a new generation of anti-mycobacterial agents.

Keywords: CYP51, cytochrome P450; *Mycobacterium tuberculosis*; Sterols; Azole antifungals; Isoniazid

1. Introduction

World Health Organization data indicate that tuberculosis is a major cause of death in developing countries [1]. The current treatment against *Mycobacterium tuberculosis*, the causative agent of tuberculosis in humans, requires a drug combination that often includes isoniazid and rifampacin [2]. The last two decades have passed without significant development of novel chemicals for the treatment of tuberculosis. In developed countries, the AIDS epidemic and the emergence of drug-resistant *M. tuberculosis* strains are causing a resurgence of this deadly disease [3]. Recently, collaborative efforts headed by investigators at the Pasteur Institute resulted in the elucidation of the sequence of genomes from various pathogens, including the *M. tuberculosis* genome [4,5]. This important work will reveal novel targets for drug development that may improve the treatment of patients that suffer debilitating infectious diseases [6]. Analysis of the *M. tuberculosis* genome identified a gene that encodes a potential target for development of anti-mycobacterial compounds. This gene encodes a protein with 34% amino acid sequence similarity to human CYP51. Because of this high similarity between the amino acid sequence of CYP51 isozymes and the predicted amino acid sequence encoded by the recently identified gene from *M. tuberculosis*, we henceforth refer to this protein as MT CYP51.

CYP51 isozymes are expressed throughout the phyla of life on earth and belong to the cytochrome P450 family of monooxygenases [7]. Mammalian and fungal CYP51 isozymes catalyze the 14α-demethylation of lanosterol, an important reaction in cholesterol and ergosterol biosynthe-

* Corresponding author. Tel. 1-860-297-2351; fax: 1-860-297-2538.
E-mail address: hebe.guardioladiaz@mail.trincoll.edu (H.M. Guardiola-Diaz)
[1]Present address: Candidate Enhancement Biology, Pfizer Central Research, Eastern Point Road, Groton, CT 06340-5146.

Abbreviations: CYP, cytochrome P450; CYP51, lanosterol-14α-demethylase; MT, *Mycobacterium tuberculosis* and PCR, polymerase chain reaction.

0006-2952/01/$ – see front matter
PII: S0006-2952(01)00571-8

sis, respectively. Plant CYP51 catalyzes demethylation of obtusifoliol in the phytosterol biosynthetic pathway [7]. A unifying trait in these diverse biological systems is that the stability and structure of their biological membranes require sterols [8]. Some azole compounds are potent anti-mycotic agents, a feature that is exploited clinically in the treatment of yeast and other fungal infections [9]. It has been firmly established that the anti-mycotic properties of azole derivatives result from their ability to inhibit CYP51 [10,11]. CYP51 inhibition reduces sterol levels, thereby weakening membrane structures and preventing cell growth. It is reasonable to hypothesize that if MT CYP51 plays a role in the *M. tuberculosis* life cycle that is comparable to that of fungal CYP51, some azole derivatives are likely to interfere with its catalytic activity and will inhibit mycobacterial growth.

To test this hypothesis, azole antifungal interactions with recombinant MT CYP51 were analyzed spectrophotometrically. A number of azole derivatives with known antifungal activity bound MT CYP51 with high affinity. We were unable to associate demethylase activity with this P450 and found that rat NADPH cytochrome P450 reductase does not form an active electron transfer complex with MT CYP51. Although this impeded our ability to establish a relationship between the observed azole antifungal binding and inhibition of the predicted sterol-14α-demethylase activity, we were able to begin to investigate the role of this cytochrome in mycobacterial growth. For this purpose we used two mycobacterial species, *M. bovis* and *M. smegmatis*, accepted models for the study of *M. tuberculosis*. In growth assays, *M. bovis* and *M. smegmatis* cells were unable to proliferate in the presence of the azole compounds that bind MT CYP51. This work could spur the development of a new generation of azole antifungal-based pharmaceutical compounds that may prove effective in the treatment of tuberculosis, perhaps even inhibiting proliferation of currently drug resistant strains of *M. tuberculosis*.

2. Materials and methods

2.1. Molecular cloning of MT CYP51

The 34,665 base pairs contained in cosmid MTCY369 (provided by S. Cole and K. Eiglmeier) include a *M. tuberculosis* (H_{37}Rv strain) *cyp51*-like gene. This cosmid served as template for oligonucleotide primer design and for PCR amplification of CYP51 DNA sequences. The 5′ oligonucleotide primer (5T, 5′-CGGGATCCATGAGCGCTGTTGCACTACCCCGGGTTTCGG-3′) contains sequences corresponding to nucleotides 7495 to 7465 in MTCY369, sequences that encode the amino terminal end of the putative CYP51 protein. The 3′ primer (3T, 5′-ATAAGAATGCGGCCGCTTAAACTCCCGTTCGCCGGCGGTAGCGCACG-3′) corresponds to nucleotides 6140 to 6170 that encode the carboxyl terminal end of the CYP51-like protein, including sequences specifying termination of translation. *Bam*HI and *Not*I recognition sites were included in the 5′ and 3′ oligonucleotide primer sequences for cloning purposes. PCR amplification reactions were catalyzed by the Taq and Pwo DNA polymerases present in the Expand High Fidelity system (Boehringer Mannheim Biochemicals) according to manufacturer's instructions. The PCR product was directionally cloned into the *Bam*HI and *Not*I sites of the expression plasmid pGEX-6P1 (Pharmacia). The resulting plasmid, GST-MT*cyp51*, therefore, contains the glutathione S-transferase sequence fused immediately upstream of the MT *cyp51* gene. The 5T/3T primer pair and/or the internal primer pair 5I (5′-CACTAGCCTACGTCGACCCG-3′)/ 3I (5′-GGCCTTGCACCTCGAACTCGC-3′) were used to PCR-amplify CYP51-like sequences from *M. bovis* and *M. smegmatis*. These reactions were conducted according to manufacturer's specifications with the sole exception that whole mycobacterial cells provided the template for amplification.

2.2. MT CYP51 expression and purification in Escherichia coli

MV1304 cells have been used previously to express rabbit CYP 2E1, 2B4, and several of their respective mutants [12–14]. Cells were made competent by $CaCl_2$ treatment and transformed with the pGEX-6P1 plasmid containing the GST-MT*cyp51* construct. Typically, cells were grown in terrific broth (1.0 L) containing ampicillin (50 μg/mL) at 37°, with vigorous shaking (250 rpm), to an optical density of 0.7 to 1.5 at 600 nm. The suspensions were cooled to 22°, and isopropyl β-D-thiogalactopyranoside (IPTG) was added to a final concentration of 1 mM. The cultures were allowed to grow at 22° under reduced shaking (70 rpm) for 18 hr or until the cultures reached an OD_{600} = 2.0. Cells were harvested by centrifugation, washed with 100 mM potassium phosphate (KPi) buffer (pH 7.4) and resuspended in 100 mM KPi containing 20% glycerol (1 g cells/10 mL of buffer, 70–80 mL final volume). A French press was used to lyse cells under high pressure. The cell lysate was centrifuged first at 10,000 *g* to remove cell debris, and then at 100,000 *g* to obtain a clear supernatant that contained all of the spectrally detectable cytochrome P450. This fraction was applied to a glutathione-Sepharose 4B affinity column (Pharmacia; 2.5 × 10 cm) equilibrated in 100 mM KPi (pH 7.4)/20% glycerol buffer. The column was washed sequentially with 5 column volumes of equilibration buffer, and 10 column volumes of 300 mM KCl in equilibration buffer, and the GST-MT CYP51 chimeric protein was then eluted from the affinity column in 100 mM KPi/300 mM KCl/20% glycerol/10mM reduced glutathione. Fractions containing $A_{418} > 0.05$ were pooled and dialyzed against 100 mM KPi (pH 7.4)/20% glycerol with three buffer changes. The purified chimeric protein was digested with PreScission Protease (Pharmacia) at 4° for 24 hr. After digestion, the sample was reapplied to a glutathione-Sepharose 4B affinity column to remove the GST ter-

minal and undigested chimeric protein. The purity and integrity of the expressed protein were determined by SDS-PAGE. Carbon monoxide spectral determinations were performed as previously described [15].

2.3. Ligand binding assays

Ligand binding spectra were obtained with purified MT CYP51. Typically, to 3 mL of MT CYP51 (5 μM) in 100 mM KPi buffer (pH 7.4)/20% glycerol was added sequentially increasing volumes of a DMSO solution of the ligand to give final ligand concentrations of 1, 2, 4, 6, 8, 10, 20, 30, 40, 50, and 60 μM. Spectra were recorded from 400 to 500 nm. Difference spectra were obtained by subtracting the spectrum of ligand-free MT CYP51 from the spectra recorded in the presence of increasing ligand concentrations. The dissociation constants were determined from Eadie Hofstee plots using the absorbance difference between λ_{max} and $\lambda_{isobestic}$ at various ligand concentrations.

2.4. Bioassays to determine the effects on growth of M. bovis *and* M. smegmatis

M. smegmatis and *M. bovis* were maintained on Middlebrook 7H10 agar plates containing Middlebrook OADC supplement at 37° in a 5% CO_2 environment. The test organisms were grown to confluency, and then were used to inoculate 32mm plates of the same medium containing the test compounds at 100, 1.0, and 0.01 μM. The test compounds dissolved in DMSO were diluted in distilled water prior to mixing in the agar medium to the appropriate concentration. Growth of the *M. smegmatis* and *M. bovis* cells in the presence of various compounds was noted after 2 or 14 days, respectively. Based upon the results obtained in the agar plate assay, a select set of compounds were tested for their ability to inhibit the growth of *M. smegmatis* in broth culture growth assays. *M. smegmatis* was grown for 72 hr in 10 mL of Middlebrook 7H9 at 37° with constant aeration. Aliquots of 100 μl each were used to inoculate 10 mL of fresh Middlebrook 7H9 broth into 125mL Nephlo flasks containing various concentrations of the test compounds. Cultures were grown with constant aeration, and the growth was monitored with a Klett-Summerson Colorimeter. When the stationary phase was reached, a sample was removed from the flask and used to inoculate a fresh Middlebrook 7H10 agar plate. The cultures were assessed for purity by the Kinyon Acid Fast staining procedure.

3. Results

3.1. Characterization of a recombinant P450 from M. tuberculosis

Fig. 1A shows the DNA sequence of the GST-MT CYP51 fusion region in the GST-MT*cyp51* plasmid, which was introduced in MV1304 cells for the production of recombinant protein. Routinely cell cultures produced between 300 and 500 nmoles of spectral P450 per liter of cell suspension (7–8 g wet weight of cell paste). Results of a typical single-step affinity purification are shown in Fig. 1B. The chimeric protein was purified to electrophoretic homogeneity (Fig. 1B, lane 3) and the PreScission protease specifically cleaves the chimeric protein at the unique expected site (Fig. 1, lane 4). The migration of the pure MT CYP51 corresponded to the predicted molecular weight, 50.9 kDa. The reduced CO spectrum of the protein shows the characteristic maximum absorbance at 450 nm (Fig. 1C), demonstrating that the recombinant protein derived from the genome sequence is indeed a cytochrome P450 protein. The cloned protein is soluble and unassociated with any membrane components. Attempts to establish a functional electron-transfer complex with rat NADPH-cytochrome P450 reductase were unsuccessful (data not shown). The model organisms *M. bovis* and *M. smegmatis* contain *cyp51*-like DNA sequences. As demonstrated in Fig. 1D, PCR amplification of *M. bovis* genomic sequences yielded a 1317 bp product when the terminal 5T/3T oligonucleotide primer pair was used (lane 1). The nucleotide sequence of this PCR product is identical to MT *cyp51* (data not shown). In contrast, PCR amplification of *M. smegmatis* sequences was not achieved with this terminal oligonucleotide primer pair (lane 2). However, as demonstrated in Fig. 1E the expected 477 bp product was amplified from *M. smegmatis* (lane 2) and *M. bovis* (lane 3) in reactions containing the internal primer pair 5I/3I. The nucleotide sequence of the DNA fragment amplified from the *M. smegmatis* genome was at least 75% identical to MT *cyp51* (data not shown).

3.2. Spectral interactions of azole antifungals with MT CYP51

As shown in panels A and B of Fig. 2, econazole and ketoconazole showed distinct type II spectral interactions with MT CYP51, having maximum absorbance at 433–435 nm. Azaconazole and furafylline also showed type II interactions; however, as shown in Fig. 2C for azaconazole, the absorbance intensity at 435 nm was extremely weak. A control experiment with DMSO at the highest concentration used in the binding assays showed no interaction with MT CYP51. Of particular interest is the unusual concentration dependence of the difference spectrum shown by econazole, ketoconazole, and azaconazole. In the concentration ranges 1–10 and 20–60 μM, azaconazole showed differences in the dissociation constants (2.1 $\pm$ 0.3 and 13.0 $\pm$ 4.6 μM, respectively). In contrast, at 1–10 and 20–60 μM econazole (6.3 $\pm$ 4.2 and 5.4 $\pm$ 1.8 μM, respectively) and ketoconazole (11.1 $\pm$ 5.0 and 18.5 $\pm$ 4.5 μM, respectively) showed no differences in their dissociation constants within the two concentration ranges. However, for econazole and ketoconazole there appeared to be a quantitative difference in the magnitude of the extinction coefficients in the two concen-

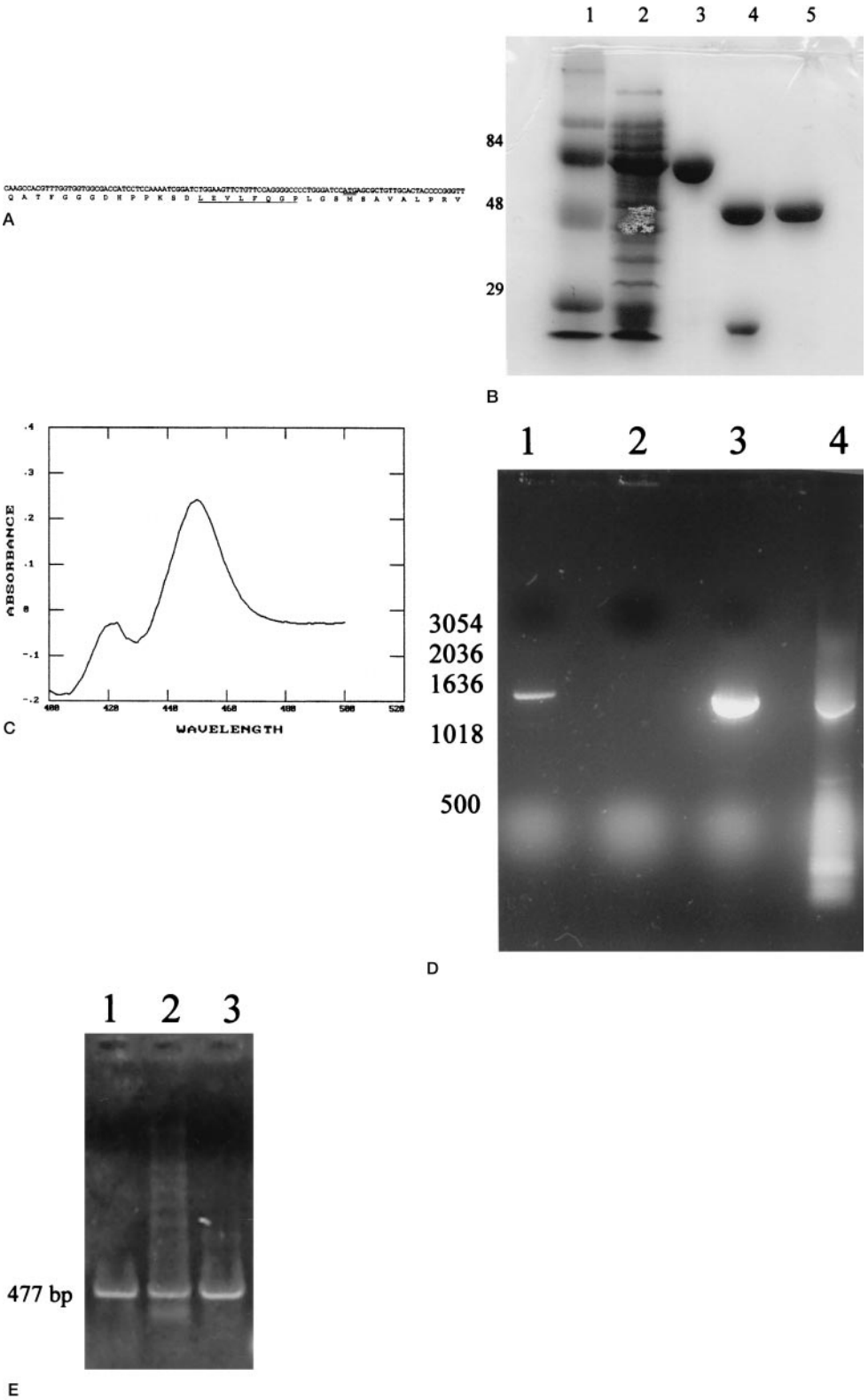

Fig. 1. MT CYP51 expression in *E. coli*. (A) The GST-P450 fusion in the GST-MT*cyp51* plasmid. The nucleotide sequence (top row) specifying the fusion between the GST and the P450 sequences is shown and the first codon in the MT CYP51 sequence is double-underlined. In the predicted amino acid sequence (bottom row) of the recombinant fusion protein, the PreScission protease recognition sequence is underlined. (B) Analysis of a one-step purification by SDS-PAGE. Lane 1, protein standards with molecular weight values kDa on the left; lane 2, 10 μg crude E. coli extract; lane 3, 5 μg pure chimeric protein; lane 4, 5 μg cleaved chimeric protein, and lane 5, 5 μg pure MT CYP51. (C) Reduced difference CO spectrum of pure MT CYP51. (D) PCR amplification of full-length mycobacterial CYP51. Lane 1, *M. bovis*; Lane 2, *M. smegmatis*; Lane 3, cosmid MTCY369; and Lane 4, *E. coli* transformed with GST-MT*cyp51*. E. PCR amplification of a mycobacterial CYP51 fragment. Lane 1, *E. coli* transformed with GST-MT*cyp51*; Lane 2, *M. smegmatis*; and Lane 3, *M. bovis*. Nucleic acid length (in bp) is indicated in the left of figures D and E.

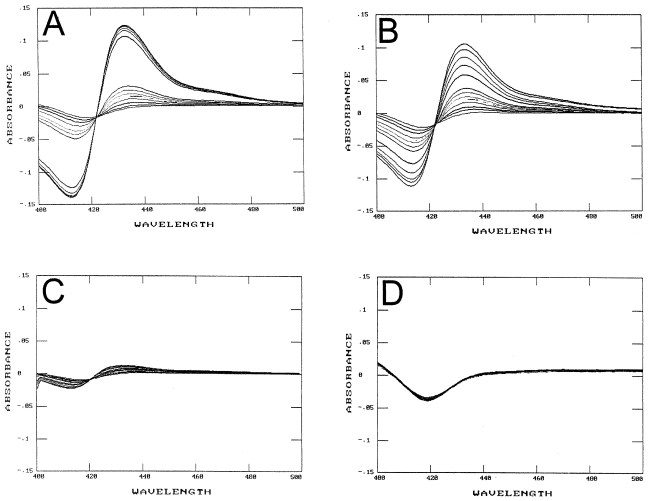

Fig. 2. MT CYP51 binding spectra. MT CYP51 spectral perturbation by addition of ligands in increments covering the 4–60 μM range. (A) econazole; (B) ketoconazole; (C) azaconazole; (D) isoniazid.

tration ranges. The significance of this difference is as yet unclear. Isoniazid demonstrated a reverse type I spectral interaction (Fig. 2D), a comparable pattern was observed with benzimidazole (data not shown). However, no dissociation constant could be obtained for either compound.

3.3. Growth inhibition of M. smegmatis *and* M. bovis

Table 1 shows the results of the plate bioassay with several azole antifungals and other CYP inhibitors. With the exception of itraconazole, metsonidazole, and terconazole all other azole compounds tested inhibited growth in both mycobacterial strains at 100 μM. By the criteria of this test, econazole was found to be the most effective inhibitor showing growth inhibition at 1.0 μM.

Azaconazole, econazole, ketoconazole, benzimidazole and furafylline were selected to further examine growth inhibition in broth culture. In these experiments, 100 μM econazole completely inhibited the growth of *M. smegmatis*, whereas ketoconazole at this concentration approximately doubled the time the organism spent in the initial lag phase of growth, and resulted in an overall decrease in the final extent of growth (Fig. 3A). Furafylline, azaconazole, and benzimidazole did not alter either the rate or the final extent of growth (Fig. 3A). To ensure that the DMSO used to dissolve the azole compounds had no effect on *M. smegmatis*, a culture containing 0.25% DMSO was included as a control and was found to have no effect on the growth of *M. smegmatis*.

The efficacy of azole antifungals as potential anti-mycobacterial agents was compared with that of isoniazid, a current therapy for tuberculosis. In a single experiment, treatment of *M. smegmatis* cultures with 5 μM isoniazid did not interfere with the growth of *M. smegmatis*, whereas at 100 μM a 36% decrease in growth was observed. In contrast, treatment with 100 μM econazole, resulted in a 100% inhibition the growth of *M. smegmatis* (Fig. 3A). This result suggests that the azole antifungals may be significantly more potent anti-mycobacterial agents than isoniazid. In experiments not shown, *M. bovis* and *M. smegmatis* cells taken from broth cultures containing azole compounds resumed normal growth on Middlebrook agar plates, indicating that these compounds are bacteriostatic agents in contrast to isoniazid, which is bacteriocidal. While we did not test the ability of these azole compounds to inhibit the growth of *M. tuberculosis* in culture, *M. bovis*, in particular, is a well-accepted model organism for the study of tuberculosis.

4. Discussion

The genome sequence of *M. tuberculosis* has revealed over 20 genes bearing CYP signature [5]. The finding that

Table 1
Azole antifungal bioassays on *M. smegmatis* and *M. bovis* growth

Compound	*M. bovis*			*M. smegmatis*		
	100 μM	1 μM	10 nM	100 μM	1 μM	10 nM
Azaconazole	−	+	+	−	+	+
Benzimidazole	+	+	+	+	+	+
Bifonazole	−	+	+	−	+	+
Clotrimazole	−	+	+	−	+	+
Econazole	−	−	+	−	−	+
Furafylline	+	+	+	+	+	+
Itraconazole	+	+	+	+	+	+
Ketaconazole	−	+	+	−	+	+
Metsonidazole	+	+	+	+	+	+
Miconazole	−	+	+	−	+	+
Nirvanol	+	+	+	+	+	+
Terconazole	+	+	+	+	+	+

Cells were grown in Middlebrook 7H9 + OADC agar plates in the presence of the compounds indicated.
Key: (+), confluent growth; and (−), growth inhibition.

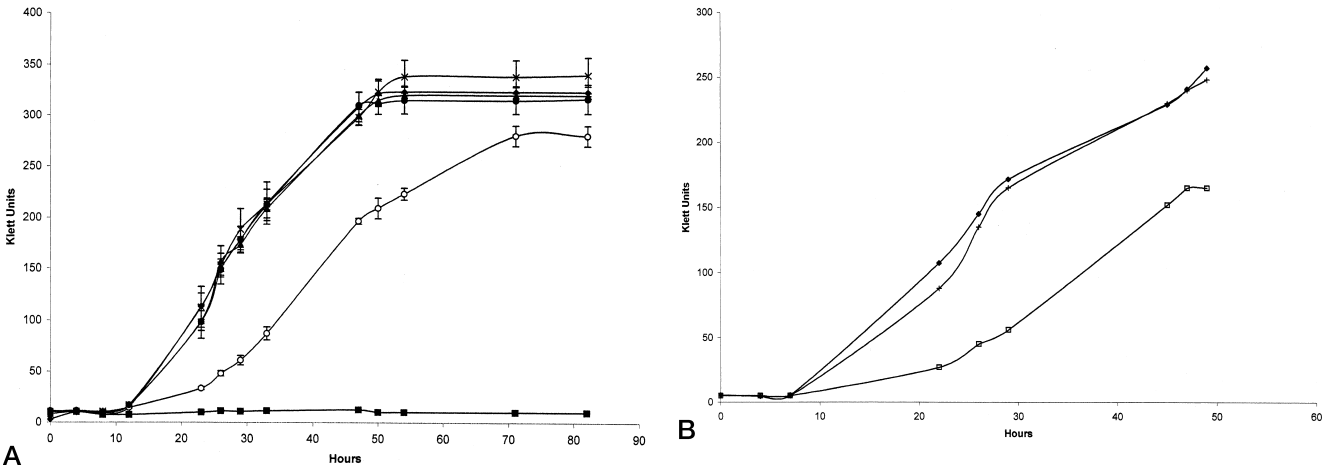

Fig. 3. *M. smegmatis* bioassays. Cultures were grown in Middlebrook 7H9 + ADC supplement liquid medium in the presence of the following treatments: (A) 0.25% DMSO control (◆); 100 μM econazole (■); 100 μM ketoconazole (○); 100 μM furafylline (●); 100 μM benzimidazole (▲); 100 μM azaconazole (★). This is a representative experiment that was performed three times, each time in triplicate. (B) Effect of isoniazid: control (◆); 5 μM isoniazid (+); 100 μM isoniazid (□).

one of these CYP sequences has 33.7% sequence identity with a mammalian lanosterol 14α-demethylase (CYP51) was remarkable because steroid biosynthesis was thought not to exist in bacteria. The laboratories of Dr. Yuzo Yoshida and Michael Waterman and our own laboratory reported the molecular cloning and expression of this novel genomic sequence in the 1998 International Congress of Cytochrome P450. Since then, Aoyama et al. [16] and Bellamine et al. demonstrated that the expressed protein is in fact a cytochrome P450 [17]. Contrary to the plant, fungal, and mammalian forms of CYP51 that are membrane bound, cloned MT CYP51 was found to be a soluble protein that did not form an active complex with NADPH cytochrome P450 reductase from the rat. Bellamine et al. [17] have demonstrated a functional complex between spinach ferrodoxin reductase, a mycobacterial iron sulfur protein, and MT CYP51 capable of demethylating dihydrolanosterol. Further identification of an endogenous substrate(s) for MT CYP51 and characterization of the reaction as it occurs *in vivo* will enhance our understanding of mycobacterial biochemistry. Interestingly, Lamb et al. [18] have recently isolated cholesterol from the membranes of *M. smegmatis* and demonstrated cholesterol biosynthesis in this organism.

Azoles that inhibit lanosterol-14α-demethylase generally show a type II spectral interaction with the enzyme. Type II spectral interactions result from coordination of a basic nitrogen with the vacant d orbitals of the heme iron. The azole antifungals examined in this study also show type II spectral interactions with MT CYP51; however, unusual bimodal binding patterns have been observed. Azaconazole shows two distinct dissociation constants for the type II spectral interaction. This suggests that there are two distinct binding sites within the heme pocket of the protein such that binding at either site permits a basic nitrogen of the ligand to co-ordinate with the heme iron with different affinities. The CYP 3A4 active site appears to contain two ligand binding sites [19], and crystallographic evidence has revealed that two androstenedione molecules bind within the P450 EryF active site [20]. MT CYP51 may also contain two binding sites in its active site. An alternative explanation is that the heme-iron co-ordinated ligand binds in different conformations within the active site, resulting in the different affinities calculated from spectral measurements. In contrast to azaconazole, which shows two dissociation constants for binding to MT CYP51, ketoconazole and econazole showed bimodality only in the intensity of the type II spectral peak (ΔA435) with no significant difference in the dissociation constants associated with the increased absorbance at 435 nm. To our knowledge such a phenomenon has not been reported previously for ligand interactions with CYP enzymes. The intensity of the type II spectral absorbance at 435 nm is dictated by the field strength of the ligand co-ordinated to the heme iron. A simple explanation for the observed results with ketoconazole and econazole may be that these ligands bind to the two binding sites within the heme pocket with comparable affinities, but the ligand field effect of the nitrogen coordinated to heme iron is stronger at one binding site, resulting in a more intense absorbance at 435 nm. Alternatively, the differences in intensity of the type II spectrum may be due to a second azole molecule that binds and enhances the ligand field effect of the first azole molecule already co-ordinated to the heme iron, thus resulting in an increase in spectral intensity without an apparent change in the dissociation constant. The other azole antifungals demonstrated weak, if any, spectral perturbations.

The effect of azole compounds on mycobacterial growth was examined in *M. bovis* and *M. smegmatis* growth assays. These two mycobacterial species are model organisms for *M. tuberculosis* that contain *cyp51*-like sequences in their genomes. Our results demonstrated that econazole and ke-

toconazole are potent inhibitors of the growth of *M. bovis* and *M. smegmatis*. In *M. bovis*, this effect was observed with econazole at concentrations as low as 500 nM (results not shown). It is difficult to explain the growth inhibition effected by azaconazole in the plate bioassay. This compound did not exhibit strong spectral perturbations and did not affect mycobacterial growth in liquid cultures. Although the purified MT CYP51 protein was used in the spectral analyses rather than the CYP51 protein from *M. bovis* or *M. smegmatis*, PCR amplification of the *M. bovis cyp*51 gene and subsequent nucleotide sequence analysis revealed that the MT *cyp51* gene and the *M. bovis cyp*51 gene are identical. A *M. smegmatis cyp*51-like genomic sequence was amplified only with internal PCR primers and is not identical to MT *cyp51*. Therefore, the *M. tuberculosis*, *M. bovis* and *M. smegmatis* CYP51 sequence identities reflect the similarities between these organisms at the organismal level. Most obviously, *M. tuberculosis* and *M. bovis* are the causative agents of identical respiratory diseases, whereas *M. smegmatis* is not a mammalian pathogen.

Our data show that the more efficacious growth-inhibiting azole compounds are those that also demonstrate the stronger spectral perturbations. It is important to note that the effects of azole compounds on cell growth are bacteriostatic. Placement of growth-inhibited cells in azole antifungal-free broth restored growth (data not shown). The important, albeit indirect, correlation between growth inhibition and binding of azole compounds to MT CYP51 suggests a possible role for MT CYP51 in the mycobacterial life cycle. The elucidation of the endogenous substrate for MT CYP51 and the establishment of a functional assay for this enzyme will conclusively determine if the azole inhibition of mycobacterial growth is a consequence of CYP51 inhibition, as occurs in fungi. Alternatively, one of the other CYP-like enzymes could be the target for the inhibitory action of the azole compounds.

Despite its bacteriostatic effect, econazole was significantly more effective than isoniazid in preventing the growth of *M. smegmatis*. Mycobacterial species are known to differ in their sensitivity to isoniazid [21]. This sensitivity results, in part, from enhanced expression of genes involved in the oxidative stress response, such as *kat*G and *ahp*C. Mycobacteria could also differ in their response to econazole, ketoconazole, and related compounds. It is therefore important to test the anti-mycobacterial properties of azole compounds in *M. tuberculosis*, an experiment that we are not able to conduct in our facilities. Azole antifungal compounds with anti-mycotic properties have been specifically tailored for topical use against fungal CYP51s [10]. The current oral use of itraconazole is encouraging [22]. At 400 mg/day, its beneficial antifungal properties outweigh any secondary side-effects caused by human CYP51 inhibition. Treatment of tuberculosis is difficult, in part, because *M. tuberculosis* avoids the immune system by residing inside macrophages. The challenge, in terms of drug development, is to design MT CYP51-specific azole derivatives that can access the pathogen without inhibiting the activity of human CYP51s. A number of cytochromes P450 have been crystallized and their three-dimensional structures have been solved. MT CYP51 is a soluble P450, a feature that distinguishes this cytochrome from other CYP51s. This feature should facilitate the determination of its structure, an ongoing effort in various laboratories. This crucial information will enhance our general understanding of lanosterol-14α-demethylase (CYP51) isozymes. Perhaps it will also expedite the development of new drugs for the treatment of tuberculosis.

References

[1] Zumla A, Mwaba P, Squire SB, Grange JM. The tuberculosis pandemic—which way now. J Infect 1999;38:74–9.

[2] Wallis RS, Patil S, Cheon SH, Edmonds K, Phillips M, Perkins MD, Joloba M, Namale A, Johnson JL, Teixeira L, Dietze R, Siddiqi S, Mugerwa RD, Eisenach K, Ellner JJ. Drug tolerance in Mycobacterium tuberculosis. Antimicrob Agents Chemother 1999;43:2600–6.

[3] Drobniewski F. Multiple drug resistant tuberculosis in the developed world. Alpe Adria Microbiol J. 1997;6:15–21.

[4] Cole S. Learning from the genome sequence of Mycobacterium tuberculosis H37Rv. FEBS Lett 1999;452:7–10.

[5] Cole ST, Brosch R, Parkhill J, Garnier T, Churcher C, Harris D, Gordon SV, Eiglmeier K, Gas S, Barry CE III, Tekaia F, Badcock K, Basham D, Brown D, Chillingworth T, Connor R, Davies R, Devlin K, Feltwell T, Gentles S, Hamlin N, Holroyd S, Hornsby T, Jagels K, Barrell BG. Deciphering the biology of Mycobacterium tuberculosis from the complete genome sequence. Nature 1998;393:537–44.

[6] Mizrahi V, Andersen SJ. DNA repair in Mycobacterium tuberculosis. What have we learnt from the genome sequence. Mol Microbiol 1998;29:1331–9.

[7] Lamb DC, Kelly DE, Kelly SL. Molecular diversity of sterol 14α-demethylase substrates in plants, fungi and humans. FEBS Lett 1998; 425:263–5.

[8] Ourisson G. The evolution of terpenes to sterols. Pure Appl Chem 1989;61:345–8.

[9] Vanden Bossche H, Dromer F, Improvisi I, Lozano-Chiu M, Rex JH, Sanglard D. Antifungal drug resistance in pathogenic fungi. Med Mycol 1998;36:119–28.

[10] Hartman PG. Inhibitors of ergosterol biosynthesis as antifungal agents. Curr Pharm Des 1997;3:177–208.

[11] Kelly S, Quali M, Rowe J, Kelly D. Sterol 14α-demethylase: target of the azole antifungal agents. In: Fernands PB, editor. New approaches for antifungal drugs, Boston: Birkehauser, 1992. p. 155–87.

[12] Vaz ADN, Pernecky SJ, Raner GM, Coon MJ. Peroxo-iron and oxenoid-iron species as alternative oxygenating agents in cytochrome P450-catalyzed reactions: switching by threonine-302 to alanine mutagenesis of cytochrome P450 2B4. Proc Natl Acad Sci USA 1996;93:4644–8.

[13] Pernecky SJ, Olken NM, Bestervelt LL, Coon MJ. Subcellular localization, aggregation state, and catalytic activity of microsomal P450 cytochromes modified in the NH2-terminal region and expressed in *Escherichia coli.* Arch Biochem Biophys 1995;318:446–56.

[14] Larson JR, Coon MJ, Porter TD. Alcohol-inducible cytochrome P-450IIE1 lacking the hydrophobic amino-terminal segment retains catalytic activity and is membrane-bound when expressed in *Escherichia coli*. J Biol Chem 1991;266:7321–4.

[15] Omura T, Sato R. The carbon monoxide-binding pigment of liver microsomes. J Biol Chem 1964;239:2379–85.

[16] Aoyama Y, Horiuchi T, Gotoh O, Noshiro M, Yoshida Y. CYP51-like gene of *Mycobacterium tuberculosis* actually encodes a P450 similar to eukaryotic CYP51. J Biochem (Tokyo) 1998;124:694–6.

[17] Bellamine A, Mangla AT, Nes WD, Waterman MR. Characterization and catalytic properties of the sterol 14α-demethylase from *Mycobacterium tuberculosis*. Proc Natl Acad Sci USA 1999;96:8937–42.

[18] Lamb DC, Kelly DE, Manning NJ, Kelly SL. A sterol biosynthetic pathway in *Mycobacterium*. FEBS Lett 1998;437:142–4.
[19] Hosea NA, Miller GP, Guengerich FP. Elucidation of distinct ligand binding sites for cytochrome P450 3A4. Biochemistry 2000;39: 5929–39.
[20] Cupp-Vickery J, Anderson R, Hatziris Z. Crystal structures of ligand complexes of P450eryF exhibiting homotropic cooperativity. Proc Natl Acad Sci USA 2000;97:3050–5.
[21] Dhandayuthapani S, Zhang Y, Mudd MH, Deretic V. Oxidative stress response and its role in sensitivity to isoniazid in mycobacteria: characterization and inducibility of ahpC by peroxides in Mycobacterium smegmatis and lack of expression in M. aurum and M. tuberculosis. J Bacteriol 1996;178:3641–9.
[22] Pierard GE, Arrese JE, Pierard-Franchimont C. Itraconazole. Expert Opin Pharmacother 2000;1:287–304.